

2.4-THz Bandwidth Optical Coherent Receiver Based on a Photonic Crystal Microcomb

Callum Deakin⁽¹⁾, Jizhao Zang^(2,3), Xi Chen⁽¹⁾, Di Che⁽¹⁾, Lauren Dallachiesa⁽¹⁾,
Brian Stern⁽¹⁾, Nicolas K. Fontaine⁽¹⁾, Scott Papp^(2,3)

⁽¹⁾ Nokia Bell Labs, 600 Mountain Ave, Murray Hill, NJ, USA callum.deakin@nokia-bell-labs.com

⁽²⁾ Time and Frequency Division, National Institute of Standards and Technology, Boulder, Colorado, USA

⁽³⁾ Department of Physics, University of Colorado, Boulder, Colorado, USA

Abstract We demonstrate a spectrally-sliced single-polarization optical coherent receiver with a record 2.4-THz bandwidth, using a 200-GHz tantalum pentoxide photonic crystal microring resonator as the local oscillator frequency comb. ©2024 The Author(s)

Introduction

It is anticipated that the increasing traffic in optical networks will precipitate a shift away from the current wavelength-routing-only paradigm^{[1],[2]}. In this scenario, scaling is achieved through both wavelength and spatial parallelism, and THz bandwidth optical superchannels are generated, routed, and detected as a single entity. This will require optical transceivers with several THz of bandwidth (or higher) while maintaining a small footprint, low cost, and low power consumption. However, current optical transceivers are limited in bandwidth to around 100 GHz, over an order of magnitude below what is required to fill the optical C-band (4.4 THz), and several orders of magnitude below the exploitable bandwidth of the optical fiber channel (>37.6 THz^[3]). The main culprits of this bandwidth limitation are the DACs and ADCs, which are both fundamentally limited by clock jitter and the switching speed of the integrated circuit technology^[4]. On the other hand, scaling through simple optical parallelism (i.e., a laser bank) makes it challenging to maintain an ultra-compact footprint and a cost-efficient solution, and results in a spectral efficiency penalty compared to fully synchronised manipulation of the optical waveform^{[5]–[7]}.

Optical frequency combs can offer solutions to these issues. Combs based on microring resonators can achieve exceptionally low timing jitter in a chip-scale footprint and can be used to build optical coherent receivers that stitch together multiple electronic sub-receivers to achieve a higher net bandwidth, bypassing the speed limitations of the electronic integrated circuits to achieve demonstrated bandwidths of up to 610 GHz^{[5],[8]–[10]}, and can be fully integrated in silicon photonics^[11]. However, conventional microcombs typically operate with pump conversion efficiencies of less than 5% and generate significant spectral content outside of the frequencies of interest^[12], which is incompatible with transceivers' strict power dissipation requirements. Furthermore, fast frequency or

power sweeps of the pump laser are required to access the soliton state due to intra-cavity thermo-optic effects, which prevent the generation of a frequency comb unless the transition to soliton state can occur much faster than the material thermal lifetime^[13]. This requires fast (MHz) control of the pump laser which adds significant design effort and complexity to the transceivers.

In this paper, we build a record high bandwidth 2.4-THz optical coherent receiver with a dark soliton microcomb generated by a dispersion-engineered photonic crystal resonator (PhCR) with a pump conversion efficiency of >20%. Unlike conventional resonator designs, the soliton state can be initiated with a simple slow (sub-Hz speed) pump frequency sweep and near unit (>86%) pump conversion efficiencies^{[14],[15]}.

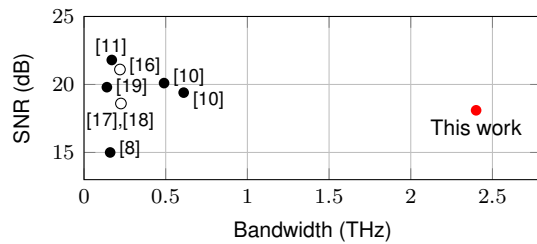


Fig. 1: High bandwidth optical coherent receiver demonstrations, including single carrier (open circles) and comb-based optical multiplexing schemes (solid circles).

Photonic crystal microring resonator

The PhCR, shown in Fig. 2(a)/(b), is fabricated in tantalum pentoxide, which offers lower residual stress, higher nonlinear index, and smaller thermo-optic coefficient compared to silicon nitride^[20]. The PhCR has normal group velocity dispersion as the dark solitons that form in this regime offer better spectral flatness and higher conversion efficiency. To control the PhCR dispersion, we design uniform ring width oscillations (see Fig. 2(b)) to induce a photonic bandgap that manifests as mode splitting at the desired resonance^[21]. The lower-frequency resonance of the split mode meets the phase-matching condition, allowing for spontaneous soli-

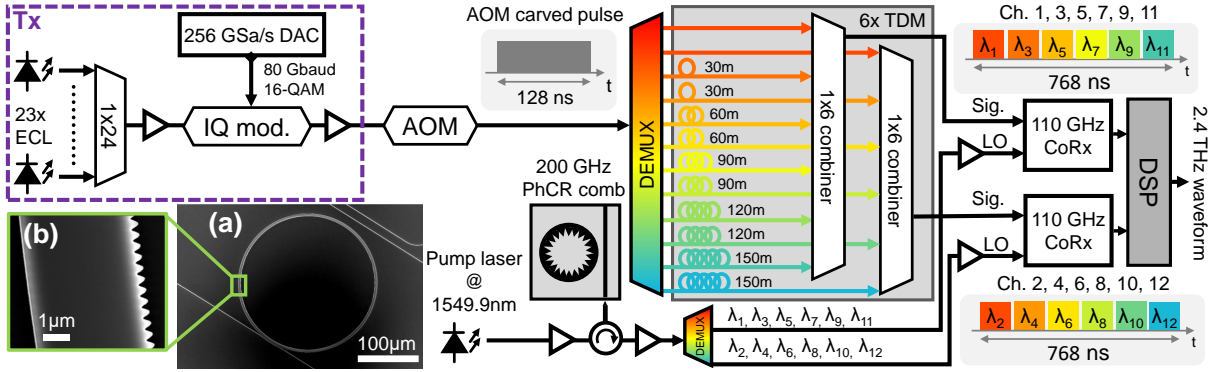


Fig. 2: Experimental setup. LO, local oscillator. Insets: scanning electron microscope (SEM) images of (a) the fabricated ring resonator and (b) detail of the ring width oscillations on the inner wall of the ring resonator.

ton formation^[22]. Solitons can then be initiated by pumping the lower-frequency resonance of the split mode, followed by a slow (sub-Hz) frequency detuning sweep of a few GHz to generate a 200-GHz spaced frequency comb centered at 193.47 THz. Unlike conventional microring combs, the generation of a soliton in our PhCR is very insensitive to the speed of the sweep because the soliton is thermally stable in the resonator, and it can be dispersion-engineered such that comb modes only appear in the desired spectral range. Light is edge-coupled in and out of the ring resonator chip via lensed fibers with coupling losses of approximately 4.5 dB/facet, which can be reduced to around 1.5 dB/facet if an oxide cladding is applied. The on-chip pump power threshold for soliton generation was measured to be 18.2 dBm, therefore the pump laser is amplified to 23 dBm to compensate for the coupling losses.

Experimental setup

The full experimental setup used to achieve a 2.4 THz detection bandwidth is shown in Fig. 2. A circulator is used to obtain the counter propagating soliton frequency comb and the observed frequency comb spectrum is shown in Fig. 3(a). The 12 comb lines indicated by the shaded area in Fig. 3(a) are used as the local oscillators for our spectrally sliced coherent receiver. The power per line varies from -0.5 dBm to -12.7 dBm after coupling to the fiber: the aggregate power of the 12 lines is 6.7 dBm (≈ 11.2 dBm on chip). At the receiver, a wavelength selective switch (WSS) is used to select and equalize the 12 comb lines. In a practical implementation, an on-chip demux device (e.g. an arrayed waveguide grating) should be used with the PhCR engineered to an even flatter power profile and equalised by on-chip attenuations instead of a WSS. Ideally, the demuxed 12 lines would be sent to 12 individual 100-GHz receivers for coherent detection. Since we do not have 12 100-GHz receivers, we emulated the required receivers through a time division multiplexing (TDM) receiver technique^[23]. The comb lines are split into two groups, the odd ($\lambda_1, \lambda_3, \dots, \lambda_{11}$)

and even channels ($\lambda_2, \lambda_4, \dots, \lambda_{12}$), which are then fed to the local oscillator ports of two 110 GHz coherent receivers with approximately 10 dBm per comb line after amplification by an erbium doped fiber amplifier (EDFA).

Meanwhile, a 2.4-THz test signal is generated by modulating 23 external cavity lasers (ECLs) with 80-Gbaud single-polarization 16-QAM signals via an IQ modulator. The ECLs are spaced at about 100 GHz and positioned such that a modulated signal is covering every channel overlap and are spread over a 2.4 THz bandwidth. To enable the TDM technique, the signal is gated into a 128-ns pulse via a 200 MHz acoustic optic modulator (AOM), which is then split into the 12×200 GHz bandwidth slices by a WSS. The 12 channels are divided into 2 groups, the odd (centered at comb lines $\lambda_1, \lambda_3, \dots, \lambda_{11}$) and even (centered at comb lines $\lambda_2, \lambda_4, \dots, \lambda_{12}$) channels, to be sent to the 2 coherent receivers operating at 256 GSa/s. The 6 channels in each group are delayed in multiples of 30 m, corresponding to a 163-ns delay. This setup allows for each coherent receiver to receive 6 simultaneously transmitted 200 GHz sub-channels each, enabling the demonstration of 12 sub-channels for a total of 2.4 THz bandwidth. Due to the TDM solution, the phase noise decorrelates slightly between consecutively received channels: we therefore use a low linewidth (< 5 kHz) laser as the comb pump laser. This is not required in a real system, provided the channels are sufficiently length-matched, so the comb can be pumped with a more typical (e.g. 100 kHz) linewidth laser.

The captured samples are upsampled offline to an aggregate sampling rate of 3.072 TSa/s and aligned by cross correlating the overlapping spectral region (12.5 GHz) of each sub-channel, as indicated by the vertical red dashed lines in Fig. 3(b), which plots the 2.4 THz bandwidth spectrum observed by the receiver. The time offset between each channel is relatively stable between captures, but can experience some drift in this experiment due to the long lengths of fiber required for the TDM technique. Each of the 80-Gbd signals is then processed via standard coherent digi-

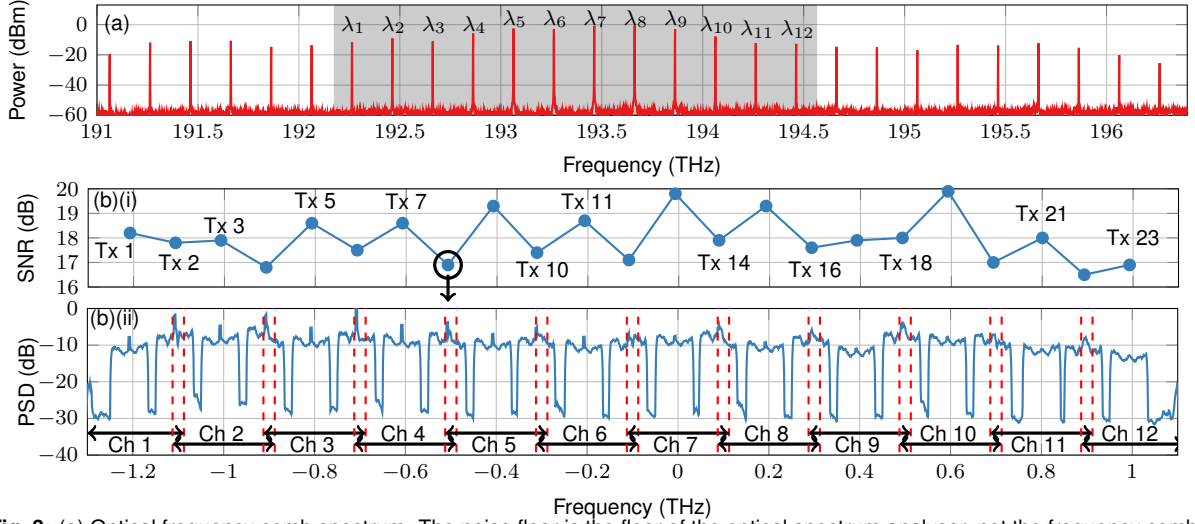


Fig. 3: (a) Optical frequency comb spectrum. The noise floor is the floor of the optical spectrum analyser, not the frequency comb. (b)(i) Received SNR and (b)(ii) 2.4 THz coherent receiver spectrum after stitching together the 12 parallel sub-channels (Ch n). Red dashed lines indicate channel edges.

tal signal processing (DSP), and a 4×2 multiple-input-multiple-output (MIMO) 801-tap least-means-squares (LMS) equaliser embedded with a digital phase locked loop. The MIMO equaliser compensates residual phase delay between both neighbouring channels and the I/Q components of the received signals^[9].

Results and Discussion

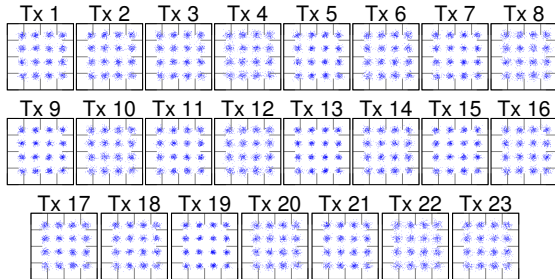


Fig. 4: Constellations for the received test channels (Tx m).

Fig. 3(b)(ii) shows the recovered 2.4 THz spectrum after restitching, with recovered SNRs from the observed 23 Tx channels plotted above in Fig. 3(b)(i). The corresponding constellations are shown in Fig. 4. The SNR varies between 16.5 dB (Tx 22) and 19.9 dB (Tx 19), with a mean SNR of 18.1 dB. Part of the SNR variation is from the transmitter EDFA nonlinearities. This is because we modulate the 23 channels with a single IQ modulator, therefore the 23 ECLs are amplified via one EDFA before the modulator, resulting in a relatively strong four-wave mixing (FWM) in the EDFA. This is an artifact of the setup and would not exist if the channels were independently generated as in a normal telecom system. Despite the Tx nonlinearity, the SNRs of the sequences that require stitching (i.e. Tx 2, 4, ..., 22) are still systematically around 1-3 dB lower than neighboring sequences that are captured fully within a signal sub-channel. This is for two reasons. Firstly, the poor roll-off and

insertion loss of the WSS used in this experiment causes significant loss and distortion at the channel overlap, which could be improved by using a specially designed arrayed waveguide grating or other on-chip demultiplexing device. Secondly, the reduced responsivity of the photodiodes at the edge of the sub-channel reduces the receiver's sensitivity in these spectral regions, which is already limited by the power damage threshold of the photodiodes, since 6 channels must be sent to each coherent receiver due to the TDM technique used in this proof of concept experiment.

Despite our non-ideal transmitters as well as the degradations brought by the TDM receiver, all the received 80-Gbd signals have an SNR of higher than 16.5 dB covering a total bandwidth of 2.4 THz, a significant improvement on the previous record of 610 GHz^[10] and the existing state of the art as plotted in Fig. 1. The worst case pre-FEC BER was observed to be 1.3×10^{-3} which is sufficient to allow error free ($< 10^{-15}$) transmission for several hard-decision FEC schemes with overheads of 6.7%^[24]. Therefore, despite zero effort to optimise the modulation format or coding for the channel, this represents a net bit rate of 6.87 Tb/s on a single polarisation, far beyond the previous record for a single polarisation coherent receiver (1.79 Tb/s^[10]). This highlights the huge potential microcombs have in scaling the capacity of a single optical receiver, enabling energy and cost efficient networks based on optical superchannels.

Conclusion

We demonstrate a record 2.4-THz bandwidth coherent receiver using a photonic crystal microring resonator in tantalum pentoxide. These PhCRs offer stable soliton formation and high efficiencies, paving the way for efficient coherent reception of THz of bandwidth in a single optical transceiver.

References

- [1] P. J. Winzer and D. T. Neilson, "From scaling disparities to integrated parallelism: A decathlon for a decade", *Journal of Lightwave Technology*, vol. 35, no. 5, pp. 1099–1115, 2017. DOI: 10.1109/JLT.2017.2662082.
- [2] R. Schmogrow, "Solving for scalability from multi-band to multi-rail core networks", *Journal of Lightwave Technology*, vol. 40, no. 11, pp. 3406–3414, 2022. DOI: 10.1109/JLT.2022.3172628.
- [3] B. J. Puttnam, R. S. Luís, I. Phillips, *et al.*, "402 Tb/s GMI data-rate OESCLU-band transmission", in *2024 Optical Fiber Communication Conference (OFC)*, 2024, Th4A.3. DOI: 10.1364/OFC.2024.Th4A.3.
- [4] R. H. Walden, "Analog-to-digital converter survey and analysis", *IEEE Journal on selected areas in communications*, vol. 17, no. 4, pp. 539–550, 1999. DOI: 10.1109/49.761034.
- [5] N. K. Fontaine, X. Liu, S. Chandrasekhar, *et al.*, "Fiber nonlinearity compensation by digital backpropagation of an entire 1.2-tb/s superchannel using a full-field spectrally-sliced receiver", in *39th European Conference and Exhibition on Optical Communication (ECOC 2013)*, 2013, Mo.3.D.5. DOI: 10.1049/cp.2013.1288.
- [6] E. Temprana, E. Myslivets, B.-P. Kuo, *et al.*, "Overcoming kerr-induced capacity limit in optical fiber transmission", *Science*, vol. 348, no. 6242, pp. 1445–1448, 2015. DOI: 10.1126/science.aab1781.
- [7] R. Sohanpal, E. Sillekens, F. M. Ferreira, R. I. Killey, P. Bayvel, and Z. Liu, "On the impact of frequency variation on nonlinearity mitigation using frequency combs", in *Optical Fiber Communication Conference*, 2023, Th1F-3. DOI: 10.1364/OFC.2023.Th1F.3.
- [8] N. K. Fontaine, R. P. Scott, L. Zhou, F. M. Soares, J. Heritage, and S. Yoo, "Real-time full-field arbitrary optical waveform measurement", *Nature Photonics*, vol. 4, no. 4, pp. 248–254, 2010. DOI: 10.1038/nphoton.2010.28.
- [9] K. Shi, E. Sillekens, and B. C. Thomsen, "246 GHz digitally stitched coherent receiver", in *2017 Optical Fiber Communication Conference (OFC)*, 2017, pp. M3D-3. DOI: 10.1364/OFC.2017.M3D.3.
- [10] D. Drayss, D. Fang, C. Füllner, *et al.*, "Non-sliced optical arbitrary waveform measurement using soliton microcombs", *Optica*, vol. 10, no. 7, pp. 888–896, 2023. DOI: 10.1364/OPTICA.484200.
- [11] D. Drayss, D. Fang, C. Füllner, W. Freude, S. Randel, and C. Koos, "Non-sliced optical arbitrary waveform measurement (OAWM) using a silicon photonic receiver chip", *Journal of Lightwave Technology*, 2024. DOI: 10.1109/JLT.2024.3378994.
- [12] C. Bao, L. Zhang, A. Matsko, *et al.*, "Nonlinear conversion efficiency in Kerr frequency comb generation", *Optics letters*, vol. 39, no. 21, pp. 6126–6129, 2014. DOI: 10.1364/OL.39.006126.
- [13] Q. Li, T. C. Briles, D. A. Westly, *et al.*, "Stably accessing octave-spanning microresonator frequency combs in the soliton regime", *Optica*, vol. 4, no. 2, pp. 193–203, 2017. DOI: 10.1364/OPTICA.4.000193.
- [14] J. Zang, S.-P. Yu, D. R. Carlson, T. C. Briles, and S. B. Papp, "Near unit efficiency in microresonator combs", in *2022 Conference on Lasers and Electro-Optics (CLEO)*, 2022, STh4F-3. DOI: 10.1364/CLEO_SI.2022.STh4F.3.
- [15] J. Zang, S.-P. Yu, H. Liu, *et al.*, "Laser-power consumption of soliton formation in a bidirectional Kerr resonator", *arXiv preprint 2401.16740*, 2024. DOI: 10.48550/arXiv.2401.16740.
- [16] B. Geiger, E. Sillekens, F. Ferreira, R. Killey, L. Galdino, and P. Bayvel, "On the performance limits of high-speed transmission using a single wideband coherent receiver", *Journal of Lightwave Technology*, vol. 41, no. 12, pp. 3816–3824, 2023. DOI: 10.1109/JLT.2023.3277624.
- [17] D. Che, X. Chen, C. Deakin, and G. Raybon, "2.4-Tb/s single-wavelength coherent transmission enabled by 114-ghz all-electronic digital-band-interleaved dacs", in *49th European Conference on Optical Communications (ECOC 2023)*, vol. 2023, 2023, pp. 1706–1709. DOI: 10.1049/icp.2023.2672.
- [18] H. Yamazaki, M. Nakamura, Y. Ogiso, *et al.*, "Single-carrier 2.5-Tb/s transmission using CSRZ-OTDM with 8×4 digital calibrator", in *49th European Conference on Optical Communications (ECOC 2023)*, vol. 2023, 2023, pp. 21–24. DOI: 10.1049/icp.2023.1837.
- [19] D. Fang, A. Zazzi, J. Müller, *et al.*, "Optical arbitrary waveform measurement (OAWM) using silicon photonic slicing filters", *Journal of Lightwave Technology*, vol. 40, no. 6, pp. 1705–1717, 2022. DOI: 10.1109/JLT.2021.3130764.
- [20] H. Jung, S.-P. Yu, D. R. Carlson, T. E. Drake, T. C. Briles, and S. B. Papp, "Tantala Kerr nonlinear integrated photonics", *Optica*, vol. 8, no. 6, pp. 811–817, 2021. DOI: 10.1364/OPTICA.411968.
- [21] E. Lucas, S.-P. Yu, T. C. Briles, D. R. Carlson, and S. B. Papp, "Tailoring microcombs with inverse-designed, meta-dispersion microresonators", *Nature Photonics*, vol. 17, no. 11, pp. 943–950, 2023. DOI: 10.1038/s41566-023-01252-7.
- [22] S.-P. Yu, D. C. Cole, H. Jung, G. T. Moille, K. Srinivasan, and S. B. Papp, "Spontaneous pulse formation in edgeless photonic crystal resonators", *Nature Photonics*, vol. 15, pp. 461–467, 2021. DOI: 10.1038/s41566-021-00800-3.
- [23] R. G. Van Uden, C. M. Okonkwo, H. Chen, H. de Waardt, and A. M. Koonen, "Time domain multiplexed spatial division multiplexing receiver", *Optics express*, vol. 22, no. 10, pp. 12668–12677, 2014. DOI: 10.1364/OE.22.012668.
- [24] E. Agrell and M. Secondini, "Information-theoretic tools for optical communications engineers", in *2018 IEEE Photonics Conference (IPC)*, 2018, MA3.1. DOI: 10.1109/IPCon.2018.8527126.